

Analysis of Coupling Coefficient Between Two UCA-OAM Antennas Based on Infinitesimal Dipole Modeling

Jaehoon Jeong ¹, Bang Chul Jung ², *Senior Member, IEEE*, and Young Dam Kim ³

Abstract—An infinitesimal dipole modeling (IDM)-based analysis method is proposed to calculate the coupling coefficient (CC) between two uniform circular array (UCA)-orbital angular momentum (OAM) antennas. The proposed method is demonstrated to be more accurate than the asymptotic expression while also being more computationally efficient compared to the method of moments (MoM)-based full-wave simulation. Moreover, the proposed method enables CC analysis between UCAs operating in different OAM modes or in the presence of misalignment. The proposed method can potentially be utilized to estimate channel coefficients electromagnetically and to design OAM communication systems.

Index Terms—Coupling coefficient analysis, infinitesimal dipole modeling, orbital angular momentum, uniform circular array.

I. INTRODUCTION

ORBITAL angular momentum (OAM) is an attractive trait that can be possessed by an electromagnetic vortex which exhibits a linear phase distribution of $il\phi$ along the beam axis with the azimuthal angle ϕ and integer mode number l where the phase changes $2\pi l$ per revolution [1]. It has been found that light beams and radio waves can carry OAM, and those with different OAM modes are spatially orthogonal to each other [2], [3]. This discovery has led to extensive exploration of the OAM wave in the field of communications [4], [5], [6], [7] as its spatial orthogonality provides an additional degree of freedom, enabling enhanced spectral efficiency and increased capacity [8], [9].

In the radio frequency domain, OAM waves can be produced by applying various methods such as spiral phase plates [10], [11], metasurfaces [12], [13], and uniform circular arrays (UCAs) [14], [15], [16]. Several research studies have explored

the coupling coefficient (CC) of OAM systems for their application in communication. Nguyen et al. defined the link budget of the UCA-OAM system based on the transfer function from the transmitter (TX) array to the receiver (RX) array [17], [18]. [19] provided the transmittance between two OAM systems using modified circle polynomials and complex plane integration. In [20], vectorial radiation patterns were utilized to express the generalized Friis equation of the UCA-OAM link.

A UCA-OAM system can be intuitively established by feeding n th of N elements of the UCA with a phase of $i2\pi l/N$, therefore OAM waves can be readily analyzed. As indicated in the literature, UCA-OAM waves are predominantly transmitted and received within the near-field region [21], [22], [23], [24], [25]. Therefore, to accurately assess the UCA-OAM communication link, it is essential to thoroughly analyze its CC in the near-field region. Infinitesimal dipole modeling (IDM) is a precise and efficient analysis method where the current distribution of an antenna is depicted by infinitesimal dipoles (IDs) [26]. A UCA-OAM antenna can be equivalently modeled by representing each array element as an ID, with its phase proportional to the azimuthal angle and the OAM mode. This facilitates an accurate and efficient analysis of the electric and magnetic fields [27]. Furthermore, S_{21} between two antennas can be directly calculated by extracting the IDs of the antennas through the IDM [28].

Based on the IDM, we propose an accurate and efficient method to analyze the CC between two UCA-OAM antennas. The proposed method allows for precise CC analysis at any distance, including the near-field region. Moreover, unlike conventional methods, the proposed method enables the calculation of CC even when the OAM modes of the TX and RX UCAs differ or when there is a misalignment between the UCAs. Besides, the proposed method is significantly more efficient than the method of moments (MoM), offering faster calculation times and eliminating the requirement for post-processing of the scattering parameters for each array element. The proposed UCA-OAM CC analysis method can provide electromagnetically accurate and efficient assessment of OAM channel coefficients; therefore, it has the potential to be employed in designing OAM communication systems.

II. PROPOSED METHOD

A TX antenna within volume V_1 and an RX antenna within V_2 in a linear, homogeneous, and isotropic medium can be equivalently represented as volume current densities \mathbf{J}_1 (A/m^2) and \mathbf{J}_2 (A/m^2), respectively. Then, the electric field \mathbf{E} (V/m)

Received 5 January 2025; revised 3 February 2025; accepted 10 February 2025. Date of publication 13 February 2025; date of current version 4 June 2025. This work was supported in part by the Ministry of Science and ICT (MSIT), Korea, through the Information Technology Research Center (ITRC) support program under Grant IITP-2024-RS-2024-00436406 supervised by the Institute for Information and Communications Technology Planning and Evaluation (IITP) and in part by the National Research Foundation of Korea (NRF) funded by the Korea Government (MSIT) under Grant NRF2022R111A3073740. (*Corresponding authors: Bang Chul Jung; Young Dam Kim.*)

Jaehoon Jeong is with the Electronics and Telecommunications Research Institute, Daejeon 34129, Republic of Korea (e-mail: jaehoon@etri.re.kr).

Bang Chul Jung is with the Department of Electrical and Computer Engineering, Ajou University, Suwon 16499, Republic of Korea (e-mail: bcjung@ajou.ac.kr).

Young Dam Kim is with the Department of Electronics Engineering, Chungnam National University, Daejeon 34134, Republic of Korea (e-mail: youngdamkim@cnu.ac.kr).

Digital Object Identifier 10.1109/LAWP.2025.3541349

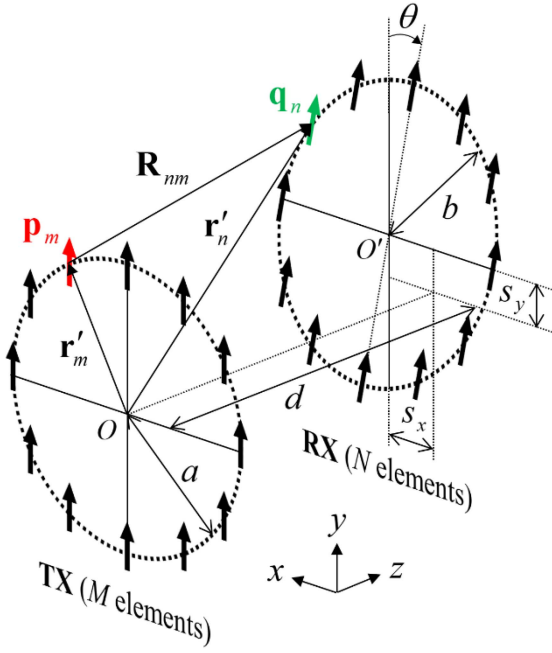


Fig. 1. TX and RX UCA-OAM antennas depicted using IDs.

radiated from the TX antenna can be described as

$$\mathbf{E}(\mathbf{r}) = \iiint_{V_1} \bar{\mathbf{G}}(\mathbf{r}, \mathbf{r}') \mathbf{J}_1(\mathbf{r}') dV_1 \quad (1)$$

where \mathbf{r} is an observation point outside V_1 and \mathbf{r}' is the position of the source within V_1 . The dyadic Green's function $\bar{\mathbf{G}}$ reflects the reaction of \mathbf{J}_1 on \mathbf{E} [27]. Based on the IDM, \mathbf{J}_1 and \mathbf{J}_2 can be alternatively expressed as electric IDs as follows:

$$\mathbf{J}_1(\mathbf{r}) = \sum_{m=1}^M \mathbf{p}_m \delta(\mathbf{r} - \mathbf{r}'_m) \quad (2)$$

$$\mathbf{J}_2(\mathbf{r}) = \sum_{n=1}^N \mathbf{q}_n \delta(\mathbf{r} - \mathbf{r}'_n) \quad (3)$$

where \mathbf{p}_m is the m th complex electric dipole moment vector at \mathbf{r}'_m and \mathbf{q}_n is the n th complex electric dipole moment vector at \mathbf{r}'_n , respectively. By substituting (2) into (1), we can express the radiated electric field as

$$\mathbf{E}(\mathbf{r}) = \frac{i}{4\pi\omega\epsilon_0} \sum_{m=1}^M \left[k^2 ((\mathbf{n}_m \times \mathbf{p}_m) \times \mathbf{n}_m) \frac{e^{ikR_m}}{R_m} + (3\mathbf{n}_m(\mathbf{n}_m \cdot \mathbf{p}_m) - \mathbf{p}_m) \left(\frac{-ik}{R_m} + \frac{1}{R_m^2} \right) \frac{e^{ikR_m}}{R_m} \right] \quad (4)$$

where ω is the angular frequency, ϵ_0 is the permittivity of free-space, k is the wavenumber, $R_m = |\mathbf{R}_m| = |\mathbf{r} - \mathbf{r}'_m|$, and $\mathbf{n}_m = \mathbf{R}_m/R_m$.

Each array element can be modeled as an electric ID for the TX and RX UCA-OAM antennas, which consist of M and N elements. As shown in Fig. 1, TX array elements are centered around the z -axis on the xy -plane and are aligned in the y -axis

direction. The TX and RX UCAs are a and b , respectively. We assume that the RX UCA is tilted by an angle θ about the x -axis according to the right-hand rule, and that the center of the RX UCA is shifted by s_x , s_y along the x - and y -axes, respectively, relative to the center of the TX UCA. In addition, the RX UCA is spaced along the z -axis by a distance of d from the TX UCA. Thus, the center of the RX is located at $O'(s_x, s_y, d)$. The OAM waves are generated by the TX UCA as each m th electric ID at $\mathbf{r}'_m(x'_m, y'_m, z'_m) = \hat{x}a \cos \phi_m + \hat{y}a \sin \phi_m$ possesses a complex dipole moment vector $\mathbf{p}_m = e^{-il\phi_m} \hat{y}$ for a TX OAM mode l , where $\phi_m = 2\pi m/M$, and \hat{x} and \hat{y} are unit x and y vector, respectively. Then, the RX UCA receives the transmitted OAM waves by having each n th electric ID at $\mathbf{r}'_n(x'_n, y'_n, z'_n) = \hat{x}(b \cos \phi_n + s_x) + \hat{y}(b \sin \phi_n \cos \theta + s_y) + \hat{z}(b \sin \phi_n \sin \theta + d)$ with a complex dipole moment vector $\mathbf{q}_n = e^{il'\phi_n} (\hat{y} \cos \theta + \hat{z} \sin \theta)$ where RX OAM mode is l' , $\phi_n = 2\pi n/N$, and \hat{z} is the unit z vector. No mutual coupling is assumed between array elements and the analysis is based on $e^{-i\omega t}$ convention. Then, the radiated electric field at \mathbf{r} is

$$\mathbf{E}(\mathbf{r}) = \frac{-i}{4\pi\omega\epsilon_0} \sum_{m=1}^M \left[\frac{e^{-i(l\phi_m - kR_m)}}{R_m^5} (k^2 R_m^2 + 3ikR_m - 3) \right] \times \left[\begin{array}{l} \hat{x}(x - x'_m)(y - y'_m) \\ + \hat{y} \left((y - y'_m)^2 - \frac{R_m^2}{3} \right) \\ - \frac{2k^2 R_m^4}{3k^2 R_m^2 + 9ikR_m - 9} \\ + \hat{z}(y - y'_m)z \end{array} \right] \quad (5)$$

Then, we can calculate the CC between the TX and RX UCA-OAM antennas as (6) by considering the effect of the electric field of the TX antenna on the current density of the RX antenna.

$$\eta = \left| \int_{V_2} \frac{\mathbf{J}_2 \cdot \mathbf{E}(\mathbf{r})}{4\sqrt{P_1 P_2}} dV_2 \right|^2 \quad (6)$$

where P_1 is the average power supplied to the TX UCA, and P_2 represents the average power delivered to the RX UCA. It is assumed that each port of the TX and RX UCA is perfectly matched. These values are derived, as explained in [28], for the power normalization of the current densities. We assume there is no mismatch at the ports of the TX and RX UCAs.

III. NUMERICAL ANALYSIS

In this section, the proposed IDM-based CC analysis is validated by comparing its results to the asymptotic formulation in [18], the Friis transmission equation, and FEKO, a method of moments (MoM)-based full-wave simulation software. The number of elements in the TX and RX UCAs is 40, i.e., $M = N = 40$, and the signal frequency is 83.5 GHz. For the MoM simulation, each element of the UCA is modeled as a short dipole with a length of $\lambda/10$, where λ is the signal's wavelength.

A. Same-Mode Analysis

We first consider a typical UCA-OAM communication scenario where $l = l'$, $s_x = s_y = 0$, and $\theta = 0$. We can represent each element as an electric ID for the RX UCA by substituting (3) into (6). Then, the CC between the TX and RX UCA-OAM

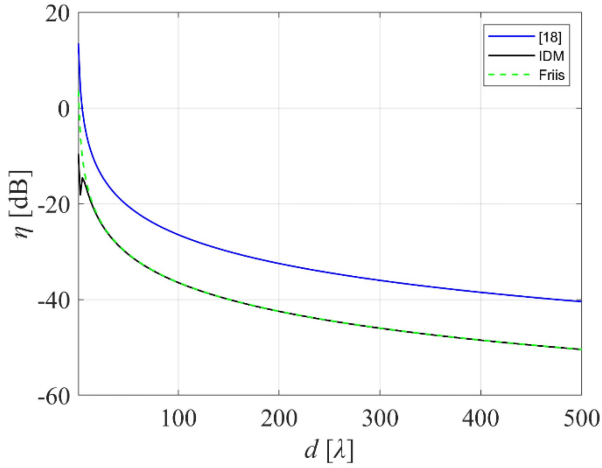


Fig. 2. Calculated CCs for $l = l' = 0$ and $a = b = 1\lambda$ based on three analysis methods.

antennas is described as

$$\eta = \left| \frac{-i}{16\pi\omega\epsilon_0\sqrt{P_1P_2}} \sum_{n=1}^N \sum_{m=1}^M \left[\frac{e^{i(kR_{nm}-l\phi_m+l'\phi_n)}}{R_{nm}^5} (k^2R_{nm}^2 + 3ikR_{nm} - 3) \left(\frac{(y'_n - y'_m)^2 - \frac{R_{nm}^2}{3}}{2k^2R_{nm}^4} \right) \right] \right|^2 \quad (7)$$

where $R_{nm} = |\mathbf{r}'_n - \mathbf{r}'_m|$ as illustrated in Fig. 1.

Fig. 2 illustrates the calculated CCs for $l = l' = 0$ and $a = b = 1\lambda$ based on the IDM, [18], and the Friis transmission equation, where d ranges up to 500λ . For the Friis transmission equation, the CC is computed using the directivity in the z -axis direction obtained from the MoM simulation. The IDM result matches the Friis equation well, while the result based on the asymptotic formulation is much larger, which is inaccurate. This occurs because the directivity calculated based on [18] exceeds the theoretical limit determined by the physical area of the UCA, as the directivity for mode 0 is estimated by simply multiplying the directivity of a single element by the number of UCA elements.

Fig. 3 depicts the calculated CCs for four OAM modes ($l = l' = 0, l = l' = 1, l = l' = 2, l = l' = 3$) and $a = b = 10\lambda$ based on the IDM, [18], and the MoM simulation, where d ranges up to 500λ . The same amount of offset is added to IDM results to observe the trend compared with the MoM results according to the distance between the UCAs. The IDM results show good agreement with the MoM results, while the results based on [18] diverge from them as d decreases from 500λ . This demonstrates that the proposed IDM-based analysis can more accurately assess the UCA-OAM link in the near-field region than the asymptotic formulation.

Furthermore, to calculate the CC of the UCA-OAM system using the MoM-based simulation, it is essential to extract the scattering parameters of all TX and RX array elements at each

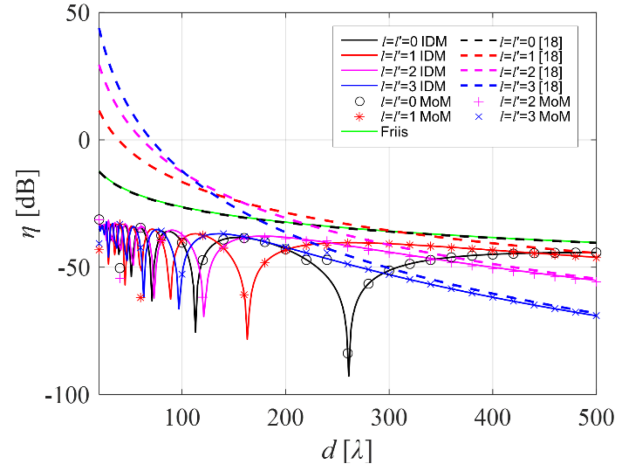


Fig. 3. Calculated CCs for four modes and $a = b = 10\lambda$ based on three analysis methods.

TABLE I
COMPUTATION TIMES OF IDM AND MoM

	IDM (proposed)	MoM
number of points (d)	251 ($d=1\lambda, 3\lambda, \dots, 501\lambda$)	25 ($d=20\lambda, 40\lambda, \dots, 500\lambda$)
computation time	0.2947 sec	7 min 26 sec

point of d . Then, the CC can be estimated as follows:

$$\eta = \left[\begin{array}{c} e^{-\frac{i2\pi l}{M}} \\ \vdots \\ e^{-\frac{i2\pi l}{M}(M-1)} \\ e^{-i2\pi l} \end{array} \right]^T \left[\begin{array}{ccc} S_{1'1} & \cdots & S_{N'1} \\ \vdots & \ddots & \vdots \\ S_{1'M} & \cdots & S_{N'M} \end{array} \right] \times \left[\begin{array}{c} e^{\frac{i2\pi l'}{N}} \\ \vdots \\ e^{\frac{i2\pi l'}{N}(N-1)} \\ e^{i2\pi l'} \end{array} \right]^2 \quad (8)$$

where the superscription T is the transpose operator. Here, the scattering parameter $S_{n'm}$ ($n = 1, 2, \dots, N, m = 1, 2, \dots, M$) denotes the ratio of the output wave of the n th port of the RX UCA divided by the input wave of the m th port of the TX UCA. The extraction and calculation process takes substantial time and computational resources. Table I compares the computation times of the IDM and the MoM for $l = l' = 1$. All computations were performed on a computer with an Intel Core i7-11700K CPU, 128 GB RAM with software FEKO 2023.1 for the MoM simulation and MATLAB R2022b for the IDM. For the MoM, the total time includes both the extraction of scattering parameters through full-wave simulation and the calculation of CCs using MATLAB. Despite processing a larger number of points, the IDM requires significantly less time, demonstrating superior computational efficiency than the MoM.

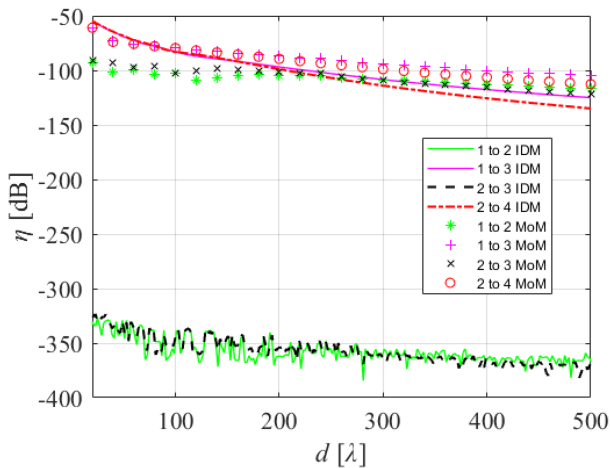


Fig. 4. Calculated CCs between different modes for $a = b = 10\lambda$ based on the IDM and the MoM-based simulation.

B. Intermode Analysis

In addition to same-mode analysis, the proposed method allows for CC analysis between two UCA-OAM systems with different OAM modes, which is not provided by previous studies. Fig. 4 depicts the CCs calculated through the proposed IDM-based method and the MoM-based simulation when the TX and RX OAM modes differ, with $s_x = s_y = 0$ and $\theta = 0$. Fig. 4 shows lower CCs for $l \neq l'$ than those for $l = l'$ in Fig. 3, illustrating mode isolation between different OAM modes.

Both the IDM and MoM results show higher CCs for $l' = l + 2$ compared to $l' = l + 1$. This is attributed to the transmission of a right-hand circularly polarized (RHCP) wave with OAM mode $l + 2$ from the TX UCA operating in mode l [29], which can be received by the RX UCA with OAM mode $l' = l + 2$. In contrast, a wave with OAM mode $l + 1$ is transmitted from the TX UCA with polarization along the z -axis, which is orthogonal to the RX UCA elements aligned along the y -axis direction, resulting in smaller CCs for $l' = l + 1$. Furthermore, all intermode MoM results are significantly higher than the IDM results of $l' = l + 1$, as the full-wave simulation accounts for realistic radiation characteristics of an actual dipole antenna, including the cross-polarization effect.

C. Misalignment Analysis

A UCA-OAM transmission system can have misalignment between the TX and RX antennas in practical scenarios. The proposed IDM-based method can provide CC analysis in the presence of misalignment, which is impossible through conventional methods. Fig. 5 portrays the CCs calculated for four OAM modes ($l = l' = 0$, $l = l' = 1$, $l = l' = 2$, $l = l' = 3$) through the proposed IDM-based method and the MoM-based simulation in case of misalignment between the TX and RX UCAs where $s_x = s_y = 0.5\lambda$ and $\theta = 3^\circ$. An offset is added to each IDM result to observe the trend compared to the MoM results according to the distance between the UCAs. The IDM results closely align with the MoM results, demonstrating that the proposed analysis can provide CC analysis even in the presence of misalignment between the TX and RX UCA-OAM antennas. Besides, even if the TX or RX UCA is tilted about any

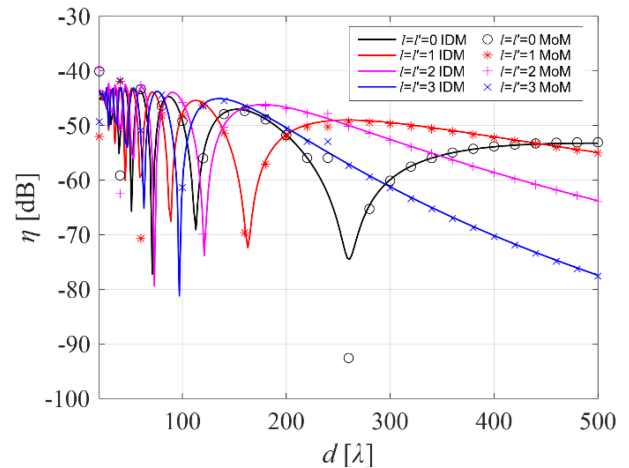


Fig. 5. Calculated CCs based on the IDM and the MoM-based simulation in the presence of misalignment ($s_x = s_y = 0.5\lambda$ and $\theta = 3^\circ$) between TX and RX.

arbitrary axis, the CC can still be evaluated using the proposed method by multiplying the ID vectors by a rotation matrix [30].

IV. CONCLUSION

This letter demonstrates the CC analysis between two UCA-OAM antennas based on the IDM. Each UCA element is modeled as an ID with a linearly increasing phase along the azimuthal angle to generate OAM waves. The coupling coefficient is calculated by accounting for the effect of the electric field radiated from the TX antenna on the IDs of the RX antenna, with power normalization of the current densities. The proposed CC analysis method is verified by comparing its results with those of the asymptotic formulation and the MoM-based simulation. The proposed method demonstrates more accurate CC analysis than the asymptotic formulation and is more computationally efficient than the MoM-based simulation. Furthermore, the proposed method can provide CC analysis even when the OAM modes of the two UCAs differ or when there is misalignment between the UCAs. The proposed method has the potential to be applied in designing OAM communication systems, as it can provide electromagnetically accurate and efficient channel coefficient analysis for such systems.

For future work, we are exploring the estimation of the CC between two OAM systems based on E-field measurements. The E-field measurement results of a real-world OAM antenna can be used to represent the antenna's current distribution as IDs through the IDM. The electromagnetic fields can then be re-radiated from the IDs to calculate CC between OAM antennas.

REFERENCES

- [1] A. Trichili, K.-H. Park, M. Zghal, B. S. Ooi, and M.-S. Alouini, "Communicating using spatial mode multiplexing: Potentials, challenges, and perspectives," *IEEE Commun. Surveys Tuts.*, vol. 21, no. 4, pp. 3175–3203, 4th Quart. 2019.
- [2] L. Allen, M. W. Beijersbergen, R. J. C. Spreeuw, and J. P. Woerdman, "Orbital angular momentum of light and the transformation of Laguerre–Gaussian laser modes," *Phys. Rev. A, Gen. Phys.*, vol. 45, no. 11, pp. 8185–8189, Jun. 1992.

- [3] F. Tamburini, E. Mari, A. Sponselli, B. Thidé, A. Bianchini, and F. Romanato, "Encoding many channels on the same frequency through radio vorticity: First experimental test," *New J. Phys.*, vol. 14, no. 3, Mar. 2012, Art. no. 033001.
- [4] Q. Wu and C. Zhang, "Orbital angular momentum backhaul link transmission based on combination of parabolic antenna and uniform circular array," *IEEE Trans. Commun.*, vol. 72, no. 8, pp. 5047–5057, Aug. 2024.
- [5] T. Hu, Y. Wang, X. Liao, J. Zhang, and Q. Song, "OFDM-OAM modulation for future wireless communications," *IEEE Access*, vol. 7, pp. 59114–59125, 2019.
- [6] W. Zhang, S. Zheng, Y. Chen, X. Jin, H. Chi, and X. Zhang, "Orbital angular momentum-based communications with partial arc sampling receiving," *IEEE Commun. Lett.*, vol. 20, no. 7, pp. 1381–1384, Jul. 2016.
- [7] R. Chen, W. Cheng, J. Lin, and L. Liang, "Cooperative orbital angular momentum wireless communications," *IEEE Trans. Veh. Technol.*, vol. 73, no. 1, pp. 1027–1037, Jan. 2024.
- [8] J. Wang et al., "Terabit free-space data transmission employing orbital angular momentum multiplexing," *Nature Photon.*, vol. 6, Jun. 2012, Art. no. 488496.
- [9] L. Wang, X. Ge, R. Zi, and C.-X. Wang, "Capacity analysis of orbital angular momentum wireless channels," *IEEE Access*, vol. 5, pp. 23069–23077, 2017.
- [10] L. Cheng, W. Hong, and Z.-C. Hao, "Generation of electromagnetic waves with arbitrary orbital angular momentum modes," *Sci. Rep.*, vol. 4, no. 1, May 2015, Art. no. 4814.
- [11] K. Miyamoto, K. Suizu, T. Akiba, and T. Omatsu, "Direct observation of the topological charge of a terahertz vortex beam generated by a tsurupica spiral phase plate," *Appl. Phys. Lett.*, vol. 104, no. 26, Jun. 2014, Art. no. 261104.
- [12] S. Yu, L. Li, G. Shi, C. Zhu, and Y. Shi, "Generating multiple orbital angular momentum vortex beams using a metasurface in radio frequency domain," *Appl. Phys. Lett.*, vol. 108, no. 24, Jun. 2016, Art. no. 241901.
- [13] H. Yang et al., "A THz-OAM wireless communication system based on transmissive metasurface," *IEEE Trans. Antennas Propag.*, vol. 71, no. 5, pp. 4194–4203, May 2023.
- [14] Y. Gong et al., "Generation and transmission of OAM-carrying vortex beams using circular antenna array," *IEEE Trans. Antennas Propag.*, vol. 65, no. 6, pp. 2940–2949, Jun. 2017.
- [15] R. Chen, W. Yang, H. Xu, and J. Li, "A 2-D FFT-based transceiver architecture for OAM-OFDM systems with UCA antennas," *IEEE Trans. Veh. Technol.*, vol. 67, no. 6, pp. 5481–5485, Jun. 2018.
- [16] A. Z. Golubović, S. V. Savić, A. Ž. Ilić, and M. M. Ilić, "Short-range transmission using OAM-carrying waves generated by uniform circular arrays," *AEU – Int. J. Electron. Commun.*, vol. 165, Jun. 2023, Art. no. 154643.
- [17] D. K. Nguyen, O. Pascal, J. Sokoloff, A. Chabory, B. Palacin, and N. Capet, "Discussion about the link budget for electromagnetic wave with orbital angular momentum," in *Proc. 8th Eur. Conf. Antennas Propag.*, The Hague, The Netherlands, Apr. 2014 pp. 1117–1121.
- [18] D. K. Nguyen et al., "Antenna gain and link budget for waves carrying orbital angular momentum," *Radio Sci.*, vol. 50, no. 11, pp. 1165–1175, Nov. 2015.
- [19] C. Craeye, "On the transmittance between OAM antennas," *IEEE Trans. Antennas Propag.*, vol. 64, no. 1, pp. 336–339, Jan. 2016.
- [20] Y. H. Cho and W. J. Byun, "Generalized Friis transmission equation for orbital angular momentum radios," *IEEE Trans. Antennas Propag.*, vol. 67, no. 4, pp. 2423–2429, Apr. 2019.
- [21] NEC, "NEC successfully demonstrates real-time digital OAM mode multiplexing transmission over 100 M in the 150 GHz-band for the first time." Accessed: Jul. 20, 2024. [Online]. Available: https://www.nec.com/en/press/202003/global_20200310_01.html
- [22] Y. Yagi, H. Sasaki, T. Yamada, and D. Lee, "200 Gb/s wireless transmission using dual-polarized OAM-MIMO multiplexing with uniform circular array on 28 GHz band," *IEEE Antennas Wireless. Propag. Lett.*, vol. 20, no. 5, pp. 833–837, May 2021.
- [23] M. I. W. Khan et al., "A 0.31-THz orbital-angular-momentum (OAM) wave transceiver in CMOS with bits-to-OAM mode mapping," *IEEE J. Solid-State Circuits*, vol. 57, no. 5, pp. 1344–1357, May 2022.
- [24] Y. Yagi, H. Sasaki, and D. Lee, "Prototyping of 40 GHz band orbital angular momentum multiplexing system and evaluation of field wireless transmission experiments," *IEEE Access*, vol. 10, pp. 130040–130047, 2022.
- [25] H. Sasaki, Y. Yagi, H. Fukumoto, and D. Lee, "OAM-MIMO multiplexing transmission system for high-capacity wireless communications on millimeter-wave band," *IEEE Trans. Wireless Commun.*, vol. 23, no. 5, pp. 3990–4003, May 2024.
- [26] S. M. Mikki and A. A. Kishk, "Theory and applications of infinitesimal dipole models for computational electromagnetics," *IEEE Trans. Antennas Propag.*, vol. 55, no. 5, pp. 1325–1337, May 2007.
- [27] J. Jeong and Y.-D. Kim, "Analysis of near-field EM energy densities for UCA-OAM wave based on infinitesimal dipoles," *IEEE Access*, vol. 12, pp. 81518–81526, 2024.
- [28] D.-J. Yun, H. Kang, I.-J. Hwang, and Y.-D. Kim, "Direct S_{21} calculation using infinitesimal dipole modeling," *IEEE Access*, vol. 11, pp. 118907–118915, 2023.
- [29] D. Liu et al., "Theoretical analysis and comparison of OAM waves generated by three kinds of antenna array," *Digit. Commun. Netw.*, vol. 7, no. 1, pp. 16–28, Feb. 2021.
- [30] S. L. Altmann, *Rotations, Quaternions, and Double Groups*. New York, NY, USA: Dover, 2005.